ELECTRIC CIRCUIT ANALYSIS FOR SHUNTED PIEZOELECTRICS

Felipe Antonio Chegury Viana
Federal University of Uberlândia, School of Mechanical Engineering
Av. João Naves de Ávila 2121 – Campus Santa Mônica – P.O. Box 593 – CEP 38400-902
Uberlândia, MG – Brazil, fchegury@mecanica.ufu.br

Valder Steffen Jr
Federal University of Uberlândia, School of Mechanical Engineering
Av. João Naves de Ávila 2121 – Campus Santa Mônica – P.O. Box 593 – CEP 38400-902
Uberlândia, MG – Brazil, vsteffen@mecanica.ufu.br

Abstract. *Structural vibrations can be attenuated through passive techniques. For this purpose, a shunted piezoelectric element bonded to a mechanical structure can be designed in such a way that a resonant circuit is obtained. Electrically, the piezoelectric behaves like a capacitor plus a controlled voltage source. Various circuit layouts for the shunt can be used. The RL topology, in series or parallel configuration, is commonly employed and since large inductances are required, synthetic inductors technology is needed. This paper is focused on the shunt circuits used in conjunction with synthetic inductors. The synthetic inductor topology is presented together with its basic ideal equations. Finally, experimental results yield a more realistic equivalent model for the synthetic inductor.*

Keywords: *passive techniques, shunted piezoelectric, synthetic inductor.*

1. INTRODUCTION

Noise and vibration suppression techniques allow the construction of more accurate medical instruments, safe buildings, more pleasant environments and more robust products. The first effect of damping in a structure is the reduction of vibration amplitudes, particularly in resonance neighborhood. This aspect implies in the reduction of stresses and fatigue, Johnson (1995).

There are active and passive techniques to obtain damping and vibration control. Actuators, power supplies and control systems characterize the active techniques. In passive techniques, the power supplies and control systems are suppressed and the shape and physical characteristics of smart materials are explored for vibration reduction.

Passive damping can be divided in two classes: structural and embedded. The structural damping occurs due the friction of junctions, cable rubbing and material damping. The embedded damping is achieved by adding dissipation mechanism to the structure, commonly based in one of four damping techniques: viscoelastic materials, viscous devices, magnetic devices and passive piezoelectrics. Table (1) shows a comparison among these approaches, Johnson (1995).

Table 1. Primary passive damping mechanisms and correlated information

	Type of damping mechanism			
	Viscoelastic materials	**Viscous devices**	**Magnetic devices**	**Passive piezoelectrics**
Type of treatment	All	Struts and TMDs*	Struts and TMDs	Strut dampers
Temperature sensitivity	High	Moderate	Low	Low
Temperature range	Moderate	Moderate	Wide	Wide
Loss factor	Moderate	High	Low	Low
Frequency range	Wide	Moderate	Moderate	Moderate
Weight	Low	Moderate	High	Moderate

(*)TMD: Tuned-Mass Damper

In this work, it is studied the case in which piezoelectric devices are associated with resonant shunt circuits, focusing in the RLC series configuration. These circuits are composed of a piezoelectric element shunted to a resistor and an inductor. In the mechanical point of view, this circuit has a similar behavior of a tuned-mass damper, as shown in several precedent works (Caruso, 2001; Fleming et al, 2002; Fleming et at, 2003; Hagood et al, 1991; Johnson, 1995; Lesieutre, 1998; Park et al, 2003; Steffen Jr. et al 1999; Wu, 1997 and Wu, 1999).

2. THE SHUNT CIRCUIT ANALYSIS

As shown in Fig. (1), the resonant shunt circuit consists of three components: an inductor L, a resistor R and a piezoelectric device PZT (lead zirconate titanate). The PZT is modeled as a controlled voltage source in series with a capacitor C_{PZT}, as shown in several references (Caruso, 2001; Fleming et al, 2002; Fleming et at, 2003; Hagood et al, 1991; Johnson, 1995; Lesieutre, 1998; Park et al, 2003; Steffen Jr. et al 1999; Wu, 1997 and Wu, 1999).

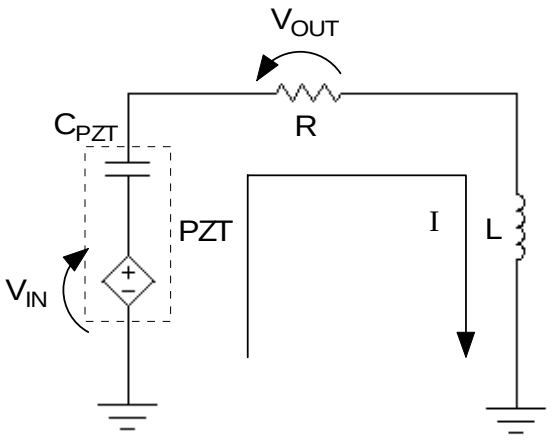

Figure 1. Scheme for the resonator shunt circuit.

The piezoelectric device is used to convert the vibration energy into electrical energy that will be dissipated via Joule effect, through the resistor R. This dissipation mechanism yields an efficient damping when the resonance frequency of the electrical circuit is tuned to the target vibration frequency of the structure.

By analyzing the electrical circuit, it is possible to obtain the transfer function H(f) that relates the voltage in the controlled voltage source and the voltage in the resistor R. V_{IN} is the voltage in the controlled voltage source and V_{OUT} is the voltage in the resistor, as shown in Fig. (1).

The electrical impedance of the circuit is given by:

$$Z_{TOTAL}(\omega) = R + jX(\omega) \tag{1}$$

$$X(\omega) = X_L(\omega) - X_{C_{PZT}}(\omega) = \omega L - \frac{1}{\omega C_{PZT}} \tag{2}$$

$$\omega = 2\pi f \tag{3}$$

where:

$Z_{TOTAL}(\omega)$: electrical impedance of the circuit
R : electrical resistance of the circuit
$X(\omega)$: electrical reactance of the circuit
$X_L(\omega)$: inductive reactance
$X_{C_{PZT}}(\omega)$: capacitive reactance (associated to the piezoelectric element)
f : electrical frequency in Hertz

By replacing Eq. (2) in Eq. (1), and using the Ohm's law:

$$H(\omega) = \frac{1}{1 + j\frac{1}{R}\left(\omega L - \frac{1}{\omega C_{PZT}}\right)} \tag{4}$$

In the resonant frequency f_0, the inductive reactance cancels the capacitive reactance and the circuit becomes purely resistive, thus implying:

$$\omega L = \frac{1}{\omega C_{PZT}} \tag{5}$$

$$f_0 = \frac{1}{2\pi\sqrt{LC_{PZT}}} \tag{6}$$

In real cases, however, two facts must be observed. First, from the mechanical point of view, the circuit behaves like a TMD, so that the resistor R must be designed to provide the optimum damping value. The second aspect is that the associated electrical frequencies are low and because of that the resonant shunt circuit requires large inductance values, such as dozens to hundreds of henries. Then, the volume and weight of the inductors would be unfeasible for passive damping purposes. This problem can be solved by using operational amplifiers to simulate the inductors, as presented in other works (Park et al 2003; Riordan, 1967; Schaumann et al, 1990; Stephenson, 1985 and Wu et al, 1997). In the literature, this type of circuit is called *gyrator* or *synthetic inductor*.

3. THE SYNTHETIC INDUCTOR

From the various types of synthetic inductors, the circuit shown in Fig. (2) is focused in this work and will be detailed in the sequence of the present contribution.

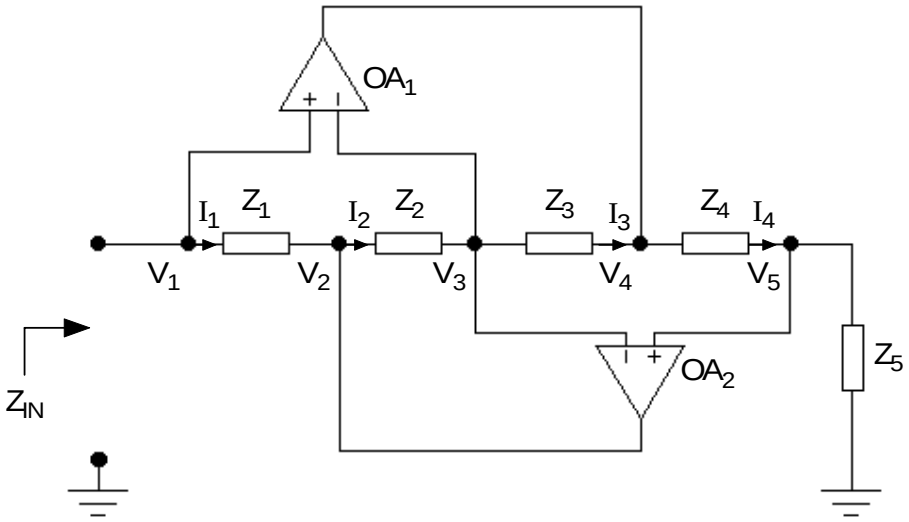

Figure 2. The synthetic inductor.

In order to analyze the circuit, without obscuring the issue with operational amplifiers nonidealities, all development is based on the ideal operational amplifiers assumption, Schaumann et al, (1990). It is assumed that the gains of the operational amplifiers are $A_1 = A_2 = \infty$, then $V_1 = V_3 = V_5$, so that:

$$I_4 = \frac{V_1}{Z_5}, \qquad V_4 = V_1\left(1 + \frac{Z_4}{Z_5}\right), \qquad I_3 = I_2 = -\frac{Z_4}{Z_3 Z_5} V_1, \tag{7}$$

$$V_2 = V_1\left(1 - \frac{Z_2 Z_4}{Z_3 Z_5}\right), \qquad I_1 = \frac{Z_2 Z_4}{Z_1 Z_3 Z_5} V_1$$

The synthetic inductor input impedance is, therefore, ideally:

$$Z_{IN} = \frac{Z_1 Z_3 Z_5}{Z_2 Z_4} \tag{8}$$

From the previous equations, a synthetic inductor is obtained by using the following relations $Z_4 = {}^{-j}\!/_{\omega C_4}$, $Z_1 = R_1$, $Z_2 = R_2$, $Z_3 = R_3$ and $Z_5 = R_5$. The equivalent circuit impedance Z_{IN} is the same as an inductor of value L_{eq}, as shown below:

$$Z_{IN} = j\omega L_{eq} \tag{9}$$

$$L_{eq} = \frac{C_4 R_1 R_3 R_5}{R_2} \tag{10}$$

Or, alternatively, by making $R_1 = R_2 = R_3 = R_5 = R$ e $C_4 = C$, one obtains:

$$L_{eq} = CR^2 \tag{11}$$

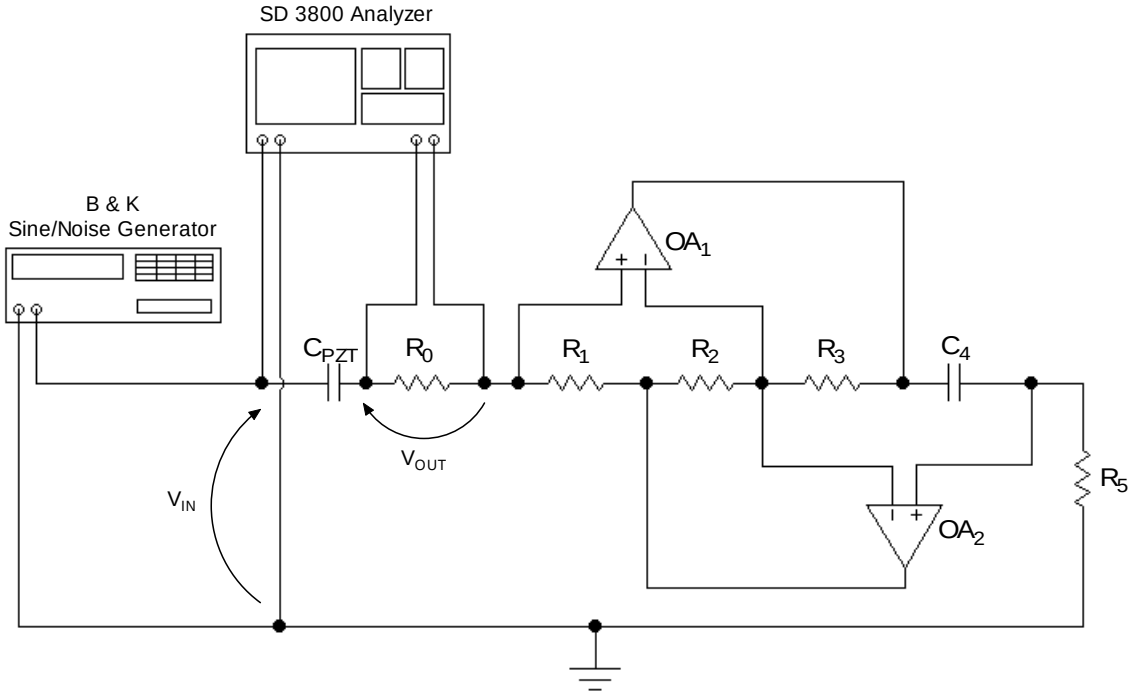

Figure 3. Experimental arrangement to test the synthetic inductor.

In order to test the performance of synthetic inductor in low electrical frequencies as typically found in mechanical systems, experiments simulating the resonant shunt circuit were performed. An RLC filter, described by Eq. (4), was configured in this experiment by using the synthetic inductor

together with a resistor R_0, a capacitor C_{PZT} and a signal generator (Brüel & Kjær Sine/Noise Generator Type 1049). A signal analyzer (Spectral Dynamics SD3800) was used to perform the frequency analysis of the circuit. The complete arrangement is shown in Fig. (3).

The signal generator introduces in the circuit a white noise of bandwidth 2Hz to 2kHz, with 1.25V of RMS value. The signals were acquired simultaneously in a sample of T = 1.6s, with intervals of dt = 0.78125ms. Then the maximum frequency analyzed is fmax = 500Hz and the frequency resolution is df = 0.6249Hz. The transfer function was estimated by using 100 samples.

The capacitor C_{PZT} and the resistor R_0 were fixed to 165.9 nF and 1.539 kΩ, respectively. Table 2 shows the values used for the remaining components along the experiments. In this case, the inductance is established according to the equation:

$$L_{eq} = \frac{1}{(2\pi f_{elet})^2 C_{PZT}} \tag{12}$$

Table 2. Experimental values of R_1, R_2, R_3, C_4 , R_5, and L_{eq}.

Experiment	R_1 [kΩ]	R_2 [kΩ]	R_3 [kΩ]	C_4 [nF]	R_5 [kΩ]	L_{eq} [H]
1	2.14	2.16	73.4	115	2.17	18.1474
2	14.66	14.76	10.86	115	14.67	18.1972
3	21.5	21.5	7.36	115	21.5	18.1976
4	99.3	99.3	1.598	115	99.1	18.2116

Fig. (4) shows the following graphics: transfer function modulus |H(f)| x f, where the gain is given in [V/V]; transfer function phase, ϕ(f) x f, where the phase is given in degrees; and the coherence between V_{IN} and V_{OUT}, γ(f) x f. In all cases the frequency is given in Hz.

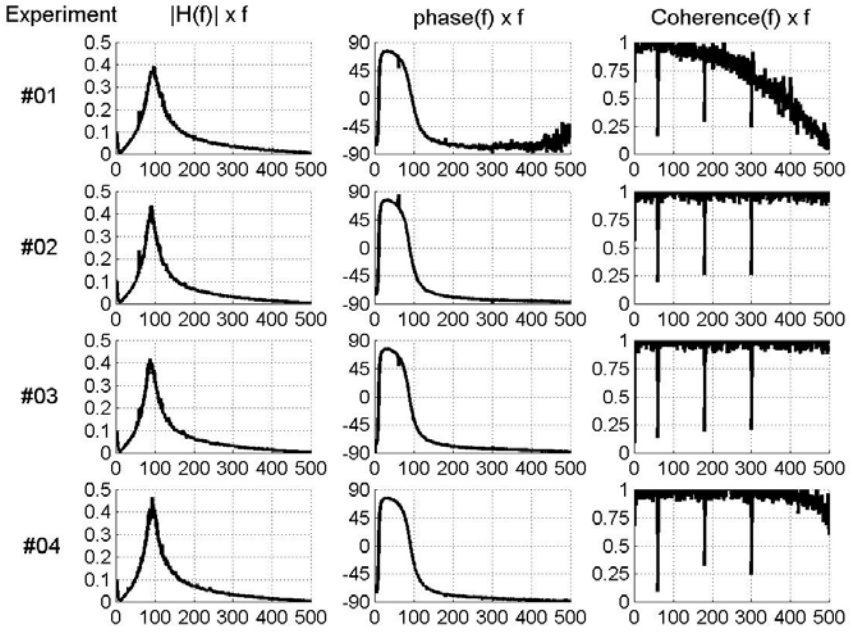

Figure 4. Experimental results of the simulated RLC filter.

In agreement with the graphics illustrated in Fig. (4), the coherence values of the experiments #01 and #04 are unsatisfactory, especially in the end of the spectrum; this probably occurs due the instable behavior of the synthetic inductor. It is important to elucidate that there is some pollution in

the electrical network that justifies the three bad values of the coherence in the frequencies equal to 60 Hz, 180Hz and 300Hz, for all experiments.

Figure (4) also shows a discrepancy between the experimental results and the analytical model adopted for the RLC circuit, as described by Eq. (4). For example, in all cases the gains are not unitary in the resonant frequency. It can be concluded that the nonidealities of the synthetic inductor generate one or more parasite resistances associated with the equivalent inductor, Park et al, 2003.

Four different configurations were tested as candidates for the equivalent circuit used in the experiments, as shown in Fig. (5).

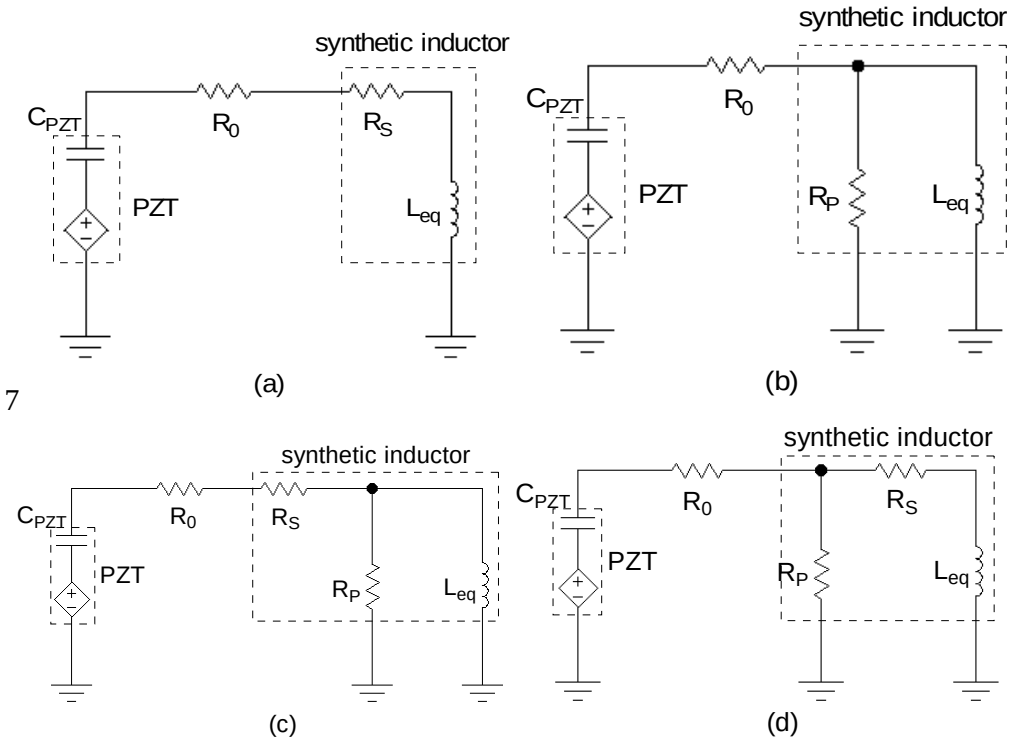

Figure 5. Candidate configurations to the synthetic inductor equivalent circuit (a) a resistor R_S in series with an inductor L_{eq}, (b) a resistor R_P in parallel with an inductor L_{eq},(c) a resistor R_P in parallel with an inductor L_{eq} and a resistor R_S in series with this branch and (d) a resistor R_S in series with an inductor L_{eq} and a resistor R_P in parallel with this branch.

The circuits shown in Fig. (5) have the transfer functions (relating the voltage in the power supply to the voltage in the resistor R_0) described below:

$$H_a(\omega) = \frac{1}{R_0 + R_S + j\left(\omega L_{eq} - \frac{1}{\omega C_{PZT}}\right)} \tag{13}$$

$$H_b(\omega) = \frac{1}{R_0 + \frac{R_p(\omega L_{eq})^2}{R_p^2 + (\omega L_{eq})^2} + j\left(\frac{(R_p)^2 \omega L_{eq}}{R_p^2 + (\omega L_{eq})^2} - \frac{1}{\omega C_{PZT}}\right)} \tag{14}$$

$$H_c(\omega) = \frac{1}{R_0 + R_S + \dfrac{R_P(\omega L_{eq})^2}{R_P^2 + (\omega L_{eq})^2} + j\left(\dfrac{(R_P)^2 \omega L_{eq}}{R_P^2 + (\omega L_{eq})^2} - \dfrac{1}{\omega C_{PZT}}\right)} \tag{15}$$

$$H_d(\omega) = \frac{1}{R_0 + \dfrac{R_P^2 R_S + R_P R_S^2 + R_P(\omega L_{eq})^2}{(R_P + R_S)^2 + (\omega L_{eq})^2} + j\left(\dfrac{(R_P)^2 \omega L_{eq}}{(R_P + R_S)^2 + (\omega L_{eq})^2} - \dfrac{1}{\omega C_{PZT}}\right)} \tag{16}$$

The experiment #03 was arbitrarily chosen to verify which from the above equations better describe the behavior of the real electrical circuit. The values of the capacitor C_{PZT} and the resistor R_0 were shown in the Tab. (2). From a curve fitting procedure, it is possible to obtain the values of R_S and R_P, as presented in Tab. (3) and Fig. (6).

Table 3. Values of R_S and R_P

Circuit Fig. (5) – (a)	Circuit Fig. (5) – (b)	Circuit Fig. (5) – (c)		Circuit Fig. (5) – (d)	
R_S [kΩ]	R_P [kΩ]	R_S [kΩ]	R_P [kΩ]	R_S [kΩ]	R_P [kΩ]
2.6480	47.9429	2.0690	192.1890	2.6480	5.3977×10^{14}

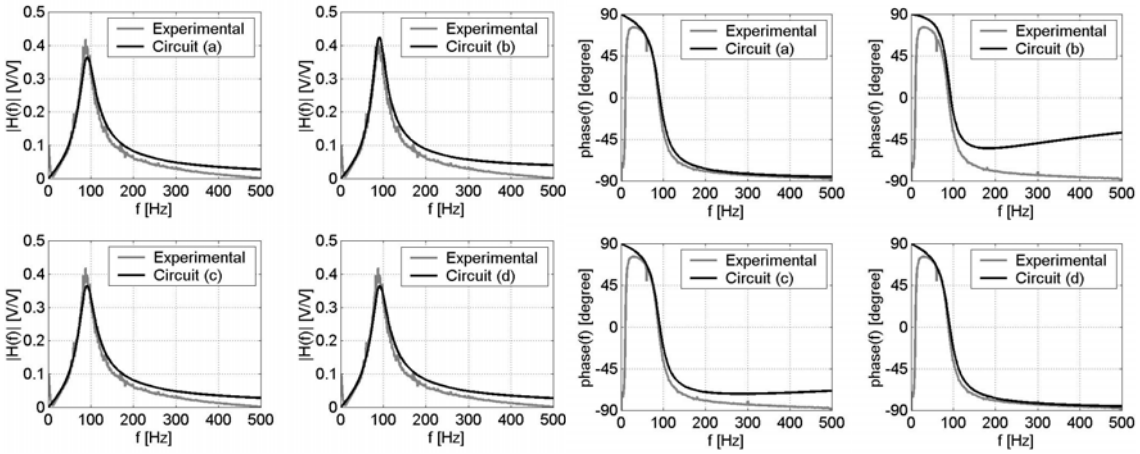

Figure 6. Transfer functions, experimental and analytical

By analyzing Tab. (3) and Fig. (6), it can be concluded that the best representation of the real electrical circuit is given by the circuit (a), where the synthetic inductor is characterized as a resistor R_S in series with an equivalent inductor L_{eq}, as described by Eq. (13). Circuit (d) presents a result very similar, however, the value of the resistor R_P is extremely high thus suggesting that R_P tends to infinite (open circuit). This characteristic leads the choice automatically to circuit (a).

4. CONCLUSION

In this paper, an electric circuit analysis was made to provide a more realistic equivalent model for the synthetic inductor. For this purpose, different analytical models were compared to experimental results. From the previous comparison, the synthetic inductor is better characterized as an inductor in series with a resistor.

The experiments also demonstrate performance variations of the synthetic inductor due to the change in its resistance values. This fact, as illustrated in Fig. (4), leads to an incoherence between the input voltage V_{IN} and the output voltage V_{OUT} of the RLC circuit, as shown in the Fig. (1).

In resonant shunt circuit applications the above aspects must be considered. First, the parasite resistance of the synthetic inductor can disable the optimum shunt configuration. Finally, the low performance of the synthetic inductor can degrade the electrical-mechanical operation of the passive damping system.

5. ACKNOWLEDMENTS

The first author is thankful to CNPQ Brazilian Research Agency for his graduate student scholarship. The second author thanks the financial support of this research work through the grant CNPq 470082/03-8).

6. REFERENCES

Caruso, G., 2001, "A critical analysis of electric shunt circuits employed in piezoelectric passive vibration damping", *Smart Materials and Structures 10*, 1059-1068.

Fleming, A. J., Behrens, S. and Moheimani, S. O. R., 2002, "Optimization and implementation of multimode piezoelectric shunt damping systems", *IEEE/ASME Transactions on Mechatronics 7*, 87-94.

Fleming, A. J., Behrens, S. and Moheimani, S. O. R., 2003, "Reducing the inductance requirements of piezoelectric shunt damping systems", *Smart Materials and Structures 12*, 57-64.

Hagood, N. W. and Von Flotow, A., 1991, "Damping of structural vibrations with piezoelectric materials and passive electrical networks", *Journal of Sound and Vibration 146*, 243-268.

Johnson, C. D., 1995, "Design of passive damping systems", *Journal of Vibration and Acoustics* 117, 171-176.

Lesieutre, G. A., 1998, "Vibration damping and control using shunted piezoelectric materials", *Shock and Vibration Digest 30*, 181-190.

Park, C. H., Inman, D. J., 2003, "Enhanced piezoelectric shunt design", *Shock and Vibration* 10, 127-133.

Riordan, R. H. S., 1967, "Simulated inductors using differential amplifiers", *Electronic Letters 3*,50-51.

Schaumann, R., Ghausi, M. S., Laker, K. R., 1990,"Design of Analog Filters: Passive, Active RC and Switched Capacitor", *Prentice Hall*.

Steffen Jr., V., Inman, D. J., 1999, "Optimal design of piezoelectric materials for vibration damping in mechanical systems", *Journal of Intelligent Material Systems and Structures 10*, 945-955.

Stephenson, F. W., 1985, "RC Active Filter Design Handbook", *Wiley Electrical and Electronics Technology Handbook Series, John Wiley & Sons*.

Wu, S. Y., Bicos, A. S., 1997, "Structural vibration damping experiments using improved piezoelectric shunts", *Proc. SPIE Smart Structures and Materials, Passive Damping and Isolation (March 1997); SPIE 3045,* 40-50.

Wu, S. Y., 1999, "Piezoelectric shunts with parallel R-L circuit for structural damping and vibration control", *Proc. SPIE Smart Structures and Materials, Passive Damping and Isolation (March 1996); SPIE 2720,* 259-269.